International Journal of Innovative Computing, Information and Control
Volume **12**, Number **3**, June **2016**

 ISSN 1349-4198
pp. 735–746

VISION CONTROL OF 5-DOF MANIPULATOR FOR INDUSTRIAL APPLICATION

Ahmed Solyman[1,*], Magdy Roman[2], Afifi Keshk[1] and Karam Sharshar[1]

[1]Radiation Engineering Department
National Center for Radiation Research and Technology
Atomic Energy Authority
Nasr City, Cairo 11787, Egypt
*Corresponding author: eng.ahmed8810@yahoo.com

[2]Mechanical Power Engineering Department
Faculty of Engineering
Helwan University
Eastern Ein Shams, Cairo 11718, Egypt
magdy_roman@m-eng.helwan.edu.eg

Received October 2015; revised March 2016

Abstract. *Computer vision is one of the growing approaches that are used to enhance robots efficiency and dexterity. The current research proposes a vision controlled arm robot to replace human operators in collecting fallen irradiative Cobalt-60 capsules inside the wet-storage pool of Cobalt-60 irradiators. A 5-DOF model robot is designed; vision control algorithm is established to pick the fallen capsules based on its color and size, record the information printed on its edge and move it to a safe storage place. A pin-hole camera model is used and its intrinsic and extrinsic parameters are identified using camera calibration techniques. Robot arm forward and inverse kinematics are developed, solved and programmed on an embedded microcontroller system. Experiments show the validity of the proposed system and prove its usefulness to replace human operators. The theoretical and experimental results show good agreement.*
Keywords: Vision controlled arm robot, RGB color filter, Pin-hole camera model, Camera calibration, Object detection, Cobalt-60 irradiator

1. **Introduction.** Robotics has proved its efficiency in nuclear and irradiation fields. In general, there have been major recent advances in robotic systems that can replace humans in many hazardous activities and dangerous environments. Such environments represent special challenges for accomplishment of the desired tasks depending on the nature and magnitude of the hazards. In nuclear fields, hazards may be present in form of radiological or toxicity dangers to potential explosions. Cobalt-60 industrial gamma irradiators are one of the important nuclear applications supported and promoted by the International Atomic Energy Agency (IAEA).

Figure 1 illustrates a typical Cobalt-60 irradiator [1], where the capsules are arranged in a source rack system that can be lifted up into the irradiation room for products processing. The irradiation room is surrounded by concrete shielding to prevent radiation exposure of operators and public. Products enter irradiation room through specially designed mazes. The source rack, when not in use, is stored near the bottom of a 5.5 m deep storage water pool. It is raised from the pool to the irradiation position by a pneumatic hoist mounted on the roof of the irradiator.

The source rack is composed of a series of Cobalt-60 capsules arranged in a specific order. One capsule is about 400 gram weight, 45.2 cm length and 11.1 mm diameter.

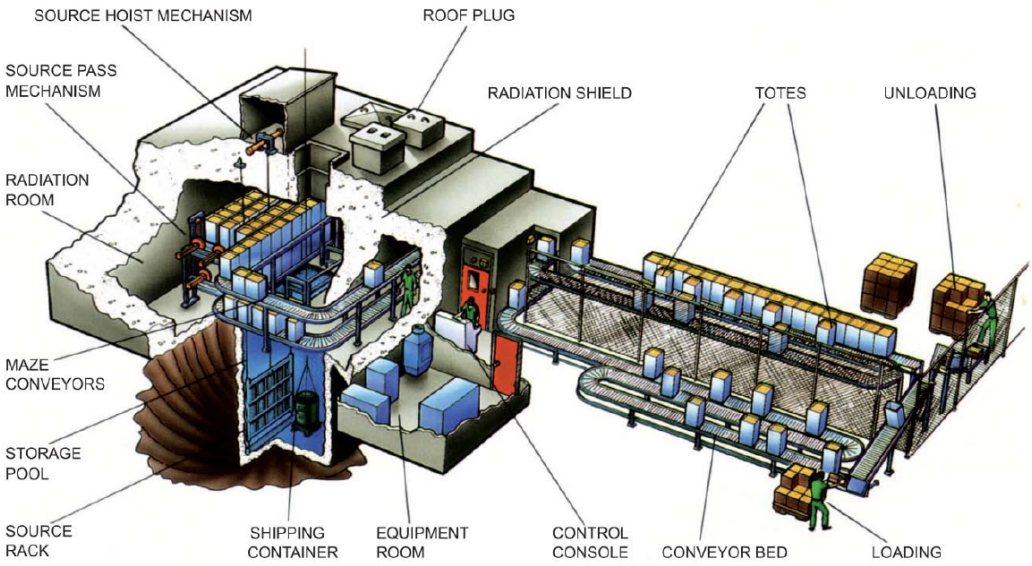

FIGURE 1. Schematic diagram of a typical panoramic, wet storage gamma industrial irradiator (courtesy of MDS Nordion-Canada) [1]

Cobalt-60 capsules have intense blue light due to Cerenkov radiation that is visible in the storage pool when the source rack is submerged [2].

Industrial Cobalt-60 irradiators have proved efficiency through successful irradiation processing. However, some major problems are recorded in different countries around the world [2]. One of these problems is the "source stuck" between source rack and horizontal product conveyors, consequently the probability of capsules falling inside the wet storage pool. The traditional methods used today to solve the mentioned problem depend on the availability of expert operators, who use special tools manually to collect the fallen capsules in the deep storage pool (about 6 m depth). These methods consume a lot of time and effort; moreover, it increases the radiation dose rate to operators. In the current research a vision-controlled 5-DOF arm robot is suggested to detect and collect the fallen capsules. According to the principle of ALARA (As Low As Reasonably Achievable) and radiation safety series [3-5], the present study is expected to increase the safety level in the Cobalt-60 irradiators.

From 1990 to 1996 the European commission conducted a research program, TELEMAN, with the aim to develop robots for use in radiation environments, in particular the nuclear power industry [6]. In 2013, the American Nuclear Society (ANS) prepared an important report containing some examples of using robotics in radiation environments such as Three Mile Island (TMI) and Fukushima nuclear power plants [7].

Machine vision has been successfully implemented in many fields such as industry, medicine, aerospace and military. In [8], vision algorithms are applied to an articulated arm robot used in in-vessel maintenance of an experimental advanced superconducting tokamak (EAST). The research presented a method of detecting and locating fragments and picking it up by using cameras installed in the scenario. In [9], a design of 7-DOF image-guided robotic system for automated venipuncture is presented. The study used near-infrared and ultra-sound imaging to guide the cannula into the selected vein under closed-loop control. The results demonstrated sub-millimeter accuracy throughout the operating workspace of the manipulator. In [10], authors presented a practical vision-based robotic bin-picking system that performs detection and 3D pose estimation of objects in an unstructured bin using a novel camera design.

To improve accuracy and performance of a vision-controlled arm robot, in [11] authors employed a visual servo technique based on template matching and forcefree control. The experimental results showed an improvement in the remote operation of the arm robot compared with other methods without visual servoing. System performance was improved in [12] through the application of active computer vision, where four bioinspired principles found in human vision system were investigated. In [13], authors addressed methodological aspects of the 3D reconstruction process of octopus arm trajectories, based on computer vision, and presented the resulting arm swimming movement of a benthic common octopus. The 3D trajectories of all eight octopus arms were tracked and analyzed, providing information about speed, acceleration and arm elongation.

Some applications of vision-controlled arm robots in nuclear field have been published during the last few years. In [14], authors developed a vision guided robotic system that rearranges the nuclear fuel pellets in a tray such that each row in the tray attains desired stack length. Nuclear fuel pellets are stacked to a fixed length before they are inserted into a tube to make a fuel pin. The proposed system used line scan cameras that can measure lengths of individual pellets to an accuracy of 100 micron. The results showed that pellets could be moved with high precision and high speed. In a similar research [15], authors developed a vision guided robotic system for measurement of fuel pellets density. The system was capable of locating, picking, placing and finally computing density by using immersive technique.

The robotic systems in [14,15], however, manipulate non-accidentally located objects. In the current study, Cobalt-60 capsules are fallen inside the wet storage pool in a random unexpected way. Both orientation and location (within the workspace) are unknown. The study suggests a design of vision controlled 5-DOF arm robot to collect the fallen capsules instead of the traditional manual method. The overall approach is described. Arm robot inverse kinematics is driven and integrated into the vision algorithms to detect fallen capsules and move them to a safe storage place. All the experiments are carried out in a dry non-radioactive environment to validate the designed system.

The rest of this paper is organized as follows. Section 2 describes the system considered in this research. In Section 3, robot forward and inverse kinematics are derived. A solution to the inverse kinematics is suggested to get the robot variables in terms of capsule location and orientation. In Section 4, proposed vision algorithms and camera calibration method are discussed. Experimental work and validating tests are illustrated in Section 5 and finally the research is concluded in Section 6.

2. **System Description.** Figure 2 describes the test rig used to accomplish the aim of the current research. The system consists of a 5-DOF arm robot in which the first joint is prismatic and the other four joints are revolute. The prismatic motion is achieved by a stepper motor (motor 1) while the revolute motions are achieved by servo-motors (motor 25). A gripper having the capability to manipulate small-size objects is attached at the end of the robot arm in such a way to facilitate moving the wrist in pitch and roll directions. The overall structure allows picking any capsule-like object at arbitrary orientation on a plane surface simulating the ground of the irradiator storage pool.

A fixed camera is used to capture the location of the objects on the ground. The images are sent to a PC of moderate-to-high processing capability for image processing and running of vision algorithms. The position and orientation of the fallen capsules are then sent to a microcontroller board based on ATmega1280 microprocessor through a 12-bit DAQ card (NI USB-6008). The microcontroller uses the robot inverse kinematic equations to generate the required signals to move the robot toward the object, pick it and move it to a safe storage area. Figure 3 shows a captured image of the fallen model

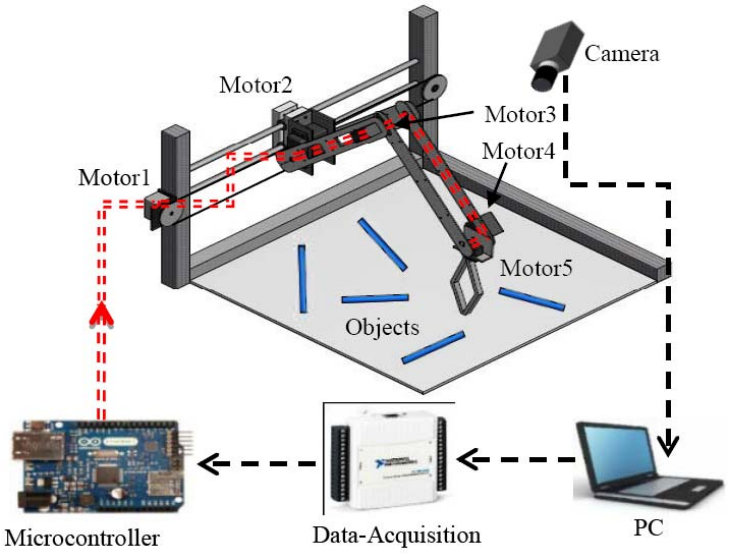

FIGURE 2. The proposed test rig

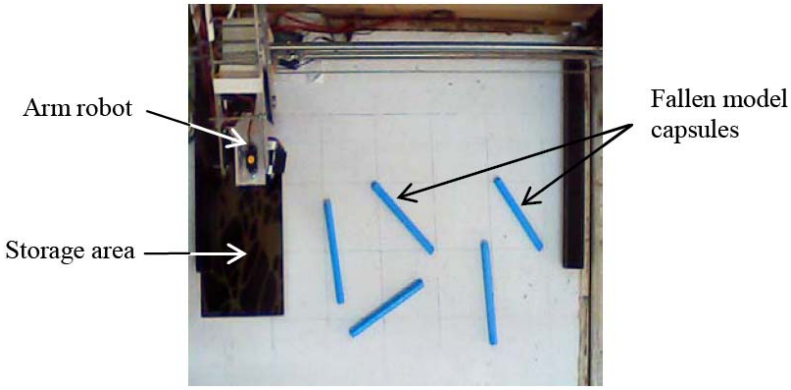

FIGURE 3. Captured image of the fallen model capsules

capsules inside the workspace using the test-rig camera. The next section discusses the forward and inverse kinematics of the proposed robotic arm and ends up with a series of equations relating the robot variables with the object position and orientation.

3. **Robot Kinematic Model.** The study of the kinematics problem can be carried out using the method of Denavit-Hartenberg (DH) [16,17]. This method is systematic in nature and suitable for modeling serial manipulators of any number of joints [18].

3.1. **Forward kinematics.** Given the link lengths and joint angles of a robotic arm, forward (direct) kinematics computes the end-effector position and orientation relative to the robot base. Figure 4 shows the frame assignment used to carry out the kinematics analysis. Frame {S} denotes the station coordinates, {0} denotes the base coordinates, {1} to {5} denote different joints coordinates, {T} denotes the tool or end-effector coordinates and finally {G} denotes the goal (object) coordinates.

Having the robot frames assigned, the robot can be described kinematically by giving the four D-H parameters for each link. Two describe the link itself, and two describe the link connection to a neighboring link in the kinematic chain [17]. The four D-H parameters are defined as:

β_{i-1} = the angle from Z_{i-1} to Z_i measured about X_{i-1} (link twist);

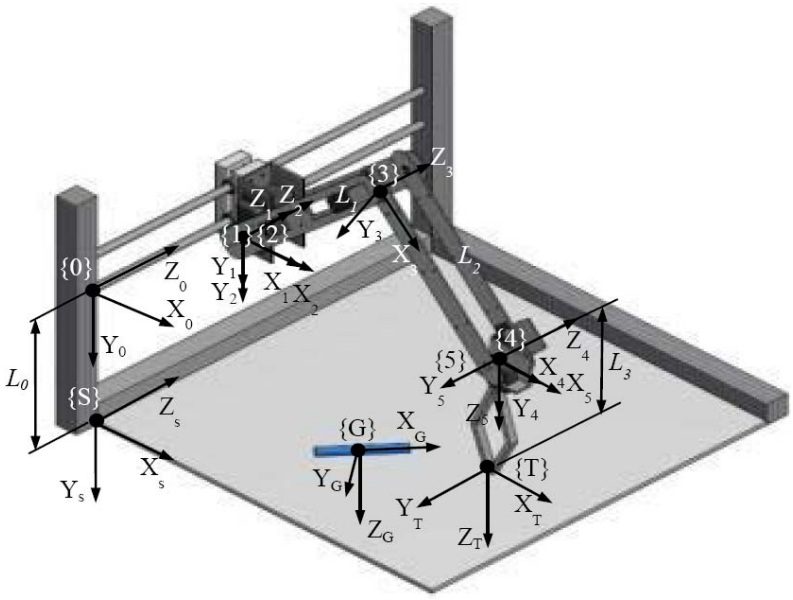

FIGURE 4. Robot frames used in the kinematic analysis

a_{i-1} = the distance from Z_{i-1} to Z_i measured along X_{i-1} (link length);
d_i = the distance from X_{i-1} to X_i measured along Z_i (link offset);
θ_i = the angle from X_{i-1} to X_i measured about Z_i (joint angle).
Table 1 shows the values of the DH parameters for the proposed robotic arm.

TABLE 1. The D-H parameters for the designed robot

i	θ_i	d_i	a_{i-1}	β_{i-1}
1	0	d_1	0	0
2	θ_2	0	0	0
3	θ_3	0	L_1	0
4	θ_4	0	L_2	0
5	θ_5	L_3	0	-90

Based on these parameters, each joint frame (i) can be expressed relative to its preceding frame $(i-1)$ using the general transformation matrix [19-21]:

$$ {}^{i-1}T_i = \begin{bmatrix} \cos\theta_i & -\sin\theta_i & 0 & a_{i-1} \\ \sin\theta_i\cos\beta_{i-1} & \cos\theta_i\cos\beta_{i-1} & -\sin\beta_{i-1} & -d_i\sin\beta_{i-1} \\ \sin\theta_i\sin\beta_{i-1} & \cos\theta_i\sin\beta_{i-1} & \cos\beta_{i-1} & d_i\cos\beta_{i-1} \\ 0 & 0 & 0 & 1 \end{bmatrix} \tag{1} $$

So,

$$ {}^0T_1 = \begin{bmatrix} 1 & 0 & 0 & 0 \\ 0 & 1 & 0 & 0 \\ 0 & 0 & 1 & 0 \\ 0 & 0 & 0 & 1 \end{bmatrix}, \quad {}^1T_2 = \begin{bmatrix} \cos\theta_2 & -\sin\theta_2 & 0 & 0 \\ \sin\theta_2 & \cos\theta_2 & 0 & 0 \\ 0 & 0 & 1 & 0 \\ 0 & 0 & 0 & 1 \end{bmatrix} $$

$$ {}^2T_3 = \begin{bmatrix} \cos\theta_3 & -\sin\theta_3 & 0 & L_1 \\ \sin\theta_3 & \cos\theta_3 & 0 & 0 \\ 0 & 0 & 1 & 0 \\ 0 & 0 & 0 & 1 \end{bmatrix}, \quad {}^3T_4 = \begin{bmatrix} \cos\theta_4 & -\sin\theta_4 & 0 & L_2 \\ \sin\theta_4 & \cos\theta_4 & 0 & 0 \\ 0 & 0 & 1 & 0 \\ 0 & 0 & 0 & 1 \end{bmatrix} $$

$$ {}^{4}T_{5} = \begin{bmatrix} \cos\theta_5 & -\sin\theta_5 & 0 & 0 \\ 0 & 0 & 1 & 0 \\ -\sin\theta_5 & -\cos\theta_5 & 0 & 0 \\ 0 & 0 & 0 & 1 \end{bmatrix} \tag{2} $$

3.2. **Inverse kinematics.** In the inverse kinematic problem the target is to find the robot variables d_1, θ_2, θ_3, θ_4 and θ_5 to bring the tool frame {T} to coincide with the goal frame {G}

$$ {}^{0}T_{5} = {}^{0}T_{1}.{}^{1}T_{2}.{}^{2}T_{3}.{}^{3}T_{4}.{}^{4}T_{5} = {}^{0}T_{S}^{S}T_{G}^{G\equiv T}T_{5}. \tag{3} $$

Given the goal position (capsules) relative to the station frame (${}^{S}T_{G}$) we can solve for the manipulator parameters through a series of algebraic equations. The closed form solution of these equations is found to be:

$$ \begin{aligned} \theta_3 &= \cos^{-1}\left(\frac{{}^{S}x_G^2 + (L_0 - L_3)^2 - (L_1^2 + L_2^2)}{2L_1L_2}\right) \\ \theta_2 &= \cos^{-1}\left(\frac{(L_0 - L_3)\ L_2\sin\theta_3 + (L_1 + L_2\cos\theta_3)\,{}^{S}x_G}{L_1^2 + L_2^2 + 2L_1L_2\cos\theta_3}\right) \\ \theta_4 &= 180 - (\theta_3 - \theta_2) \\ \theta_5 &= \psi \\ d_1 &= {}^{S}z_G \end{aligned} \tag{4} $$

where, L_0, L_1, L_2 and L_3 are link lengths; ${}^{S}x_G$ ${}^{S}z_G$ and ψ are the capsule position and orientation (roll angle of {G}) relative to frame {S}. The unknown values of ${}^{S}x_G$, ${}^{S}z_G$ and ψ are determined using proper vision algorithms and an accurate camera model. The next section describes this in more detail.

4. **Vision Guidance for Target Detection.** As has been mentioned in Section 1, the traditional way of collecting the fallen capsules in the deep storage pool is time and effort consuming and can increase the operator's radiation dose. The real contribution of the current research is that, it proposes a new technique to collect the fallen capsules without human direct intervention by using a vision-controlled arm robot. The intense blue light (due to Cerenkov radiation), which is visible in the storage pool, can be exploited to distinguish the fallen capsules. Figure 5 depicts the flow of data by which the robot is controlled.

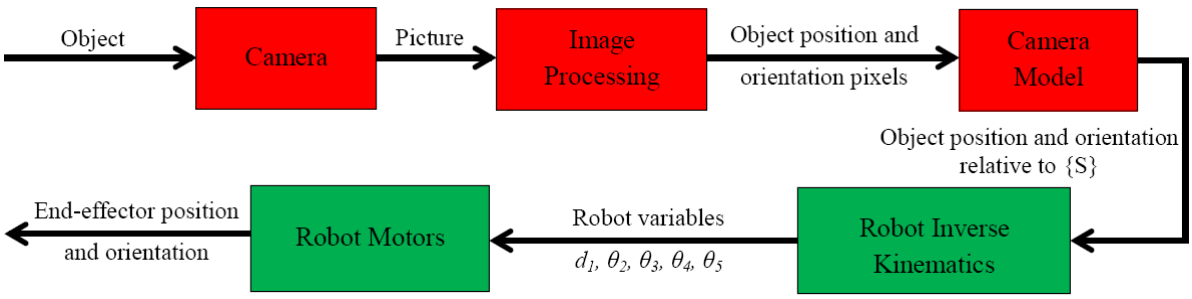

FIGURE 5. Block diagram of the vision controlled robot arm

4.1. **Calibration of the test rig camera.** In the vision-based control system camera calibration is the key step of deciding the precision. The main purpose of camera calibration is to establish the relevant coordinate system and get relationship model between image coordinate and space coordinate systems [22]. According to a corresponding relationship between calibrating points (known points in the space coordinates) and their corresponding position in the image coordinates, calibration process calculates the camera intrinsic and extrinsic parameters [23]. The study adopts the pinhole camera model to form the calibration equations and MATLAB camera calibrator toolbox is used to extract the camera extrinsic and intrinsic parameters [24,25]. The calibration technique uses some reference images (at least 3) of the chosen calibrating points to develop the data base required in the calibration process [26]. A high-quality checkerboard is usually used to provide such calibrating points. Figure 6 shows the images which are used during the calibration process. According to the corresponding relationship between characteristic points, the (pixel – mm) governing equations are found to be:

$$\begin{aligned} {}^{S}x_G &= 1.16x_{image} - 138.05 \\ {}^{S}z_G &= 1.16z_{image} - 159.53 \end{aligned} \tag{5}$$

where x_{image} and z_{image} are the capsule position in the image coordinates measured in pixel.

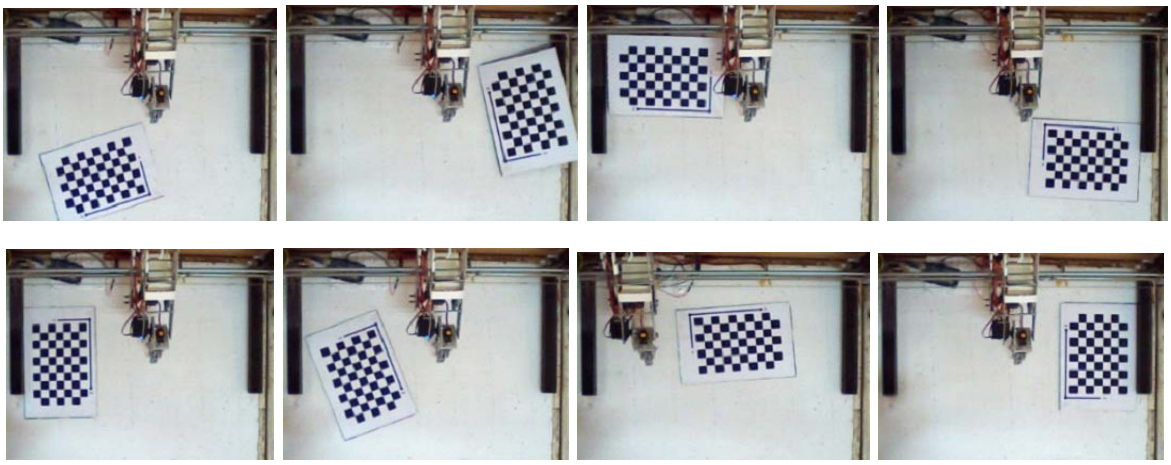

FIGURE 6. Captured images of a checkerboard pattern at different orientations relative to the camera

4.2. **Vision algorithm.** The proposed algorithm should guide the gripper to grasp the random oriented fallen objects. To accomplish the task, first, objects of interest in the captured images must be detected through a proper object detection mechanism. Then, important features of the detected objects are extracted and used to feed the robot kinematics. In the current research we investigate RGB-based filter to detect the target objects. The Blob analysis of the MATLAB computer vision toolbox is then used to measure important object properties such as area, centroid, bounding box and orientation. Description of the proposed Simulink models is given in the following part.

Object detection through RGB-based filter. The Simulink model for this algorithm is described in Figure 7. It mainly consists of two steps, first, extracting objects which have a pre-specified RGB values, in this case for the Cobalt-like color, then, using the Blob analysis to determine the detected object properties. For the RGB identification, color

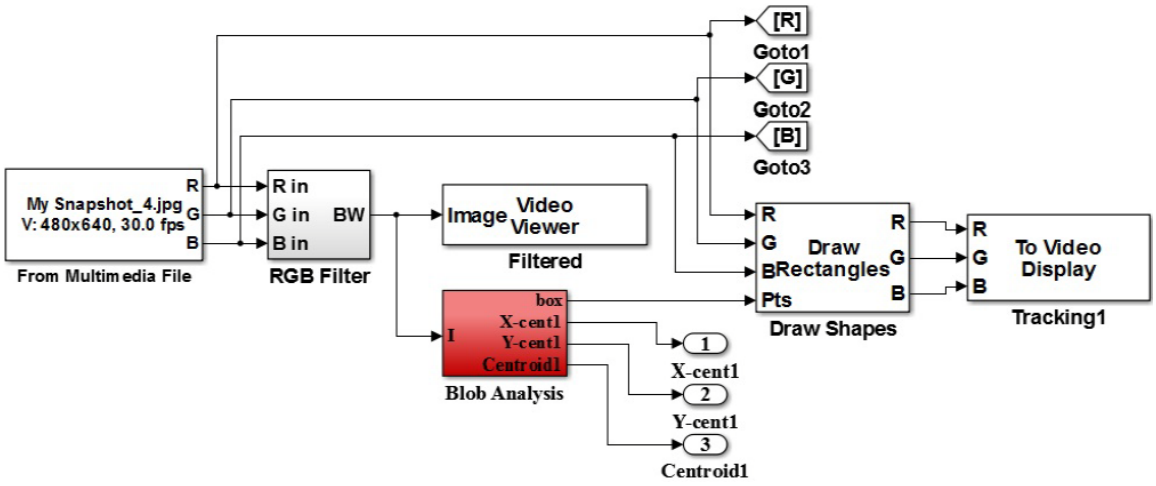

FIGURE 7. Simulink block diagram of the vision algorithm based on RGB-filter

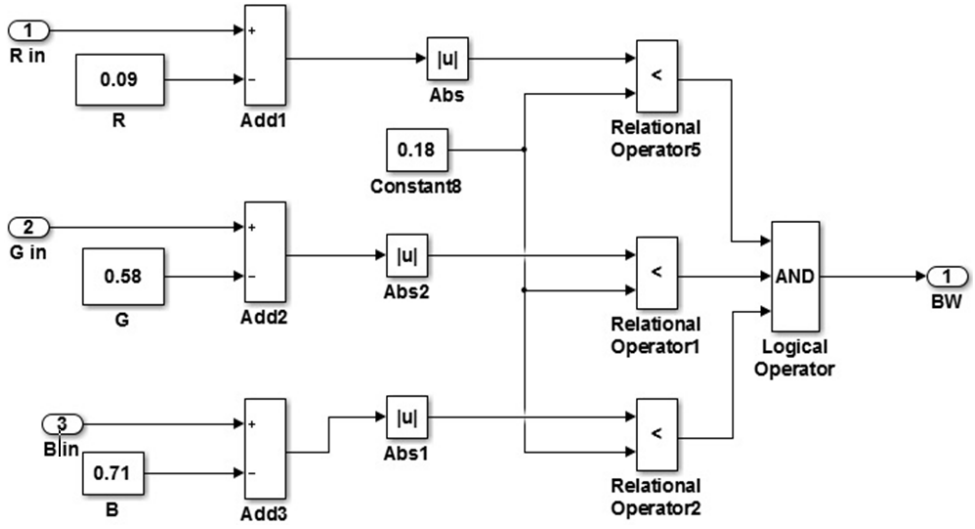

FIGURE 8. The RGB-based filter subsystem model

analyzer program is used to identify the Cobalt-like RGB values; they are found to be 0.09, 0.58 and 0.71 for red, green and blue respectively.

The RGB filter subtracts the Cobalt color RGB values from the RGB of each pixel in the image, as illustrated in the subsystem shown in Figure 8. The values of the RGB subtraction are then compared with a threshold number to convert the image to a binary image (B/W) of the detected objects only. The black and white (B/W) image is then passed to the Blob analysis block, shown in Figure 9, in order to obtain the objects boundary box, centroid and area. An important condition is set to the area that is, only objects with area between 1000 to 1500 pixels are identified. This is done to avoid shadows and other light reflections to be identified.

5. **Experimental Work.** The system described in Section 2 and shown in Figure 10 is used to validate the proposed robotic system. The previously studied algorithm is implemented to control the 5-DOF robotic arm using independent joint control mechanism. Each capsule position and orientation (${}^{S}x_G$, ${}^{S}z_G$ and ψ) are determined using the Blob analysis and the calibrated camera then inverse kinematics is solved to get the values of

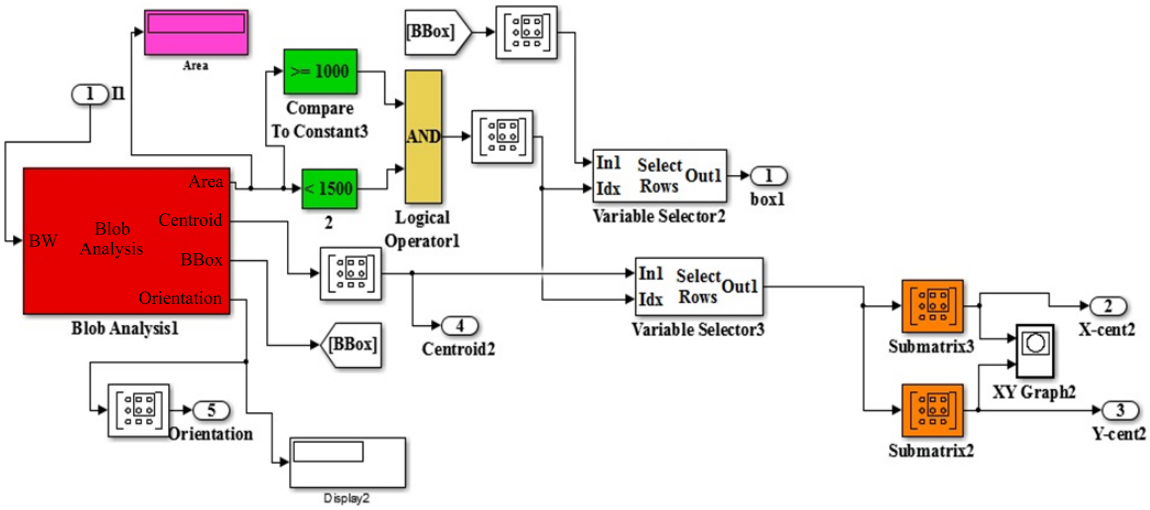

FIGURE 9. Simulink block diagram Blob analysis

FIGURE 10. Experimental test rig with robot arm in home position

the corresponding joint variables. These values are then fed to the robot motors with an adequate rate.

5.1. **Object detection.** After capturing the image as shown in Figure 3 (pre-image processing), the target objects are filtered out using the proposed RGB filter algorithm. Figure 11 shows the filtered objects as a B/W image, while Figure 12 shows colored pictures of the identified objects with a black box drawn around each detected object. Table 2 shows the position and orientation of each object and the corresponding robot variables (θ_2, θ_3, θ_4, θ_5 and d_1) determined by solving the inverse kinematics.

5.2. **Grasping object.** After detecting all the fallen objects and solving the inverse kinematics, the robot is ordered to pick the objects and place them in the storage place. Figure 13 shows the movement sequence (a)-(k) of the robot. As can be seen in (a) and (b) the robot arm moves in Z_0-direction a prismatic distance (${}^S z_G$). In (c) and (d) the arm moves to pick the object, and in (e)-(j), the object is elevated by the arm to capture the data printed on its edge and then moved to the storage place. Finally the arm returns back to home position. In (k) the arm is directed to a next object and so on.

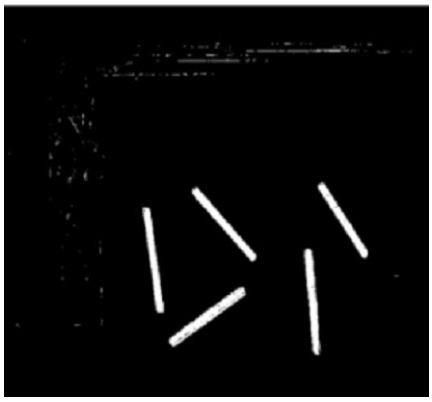

FIGURE 11. The filtered image using RGB algorithm

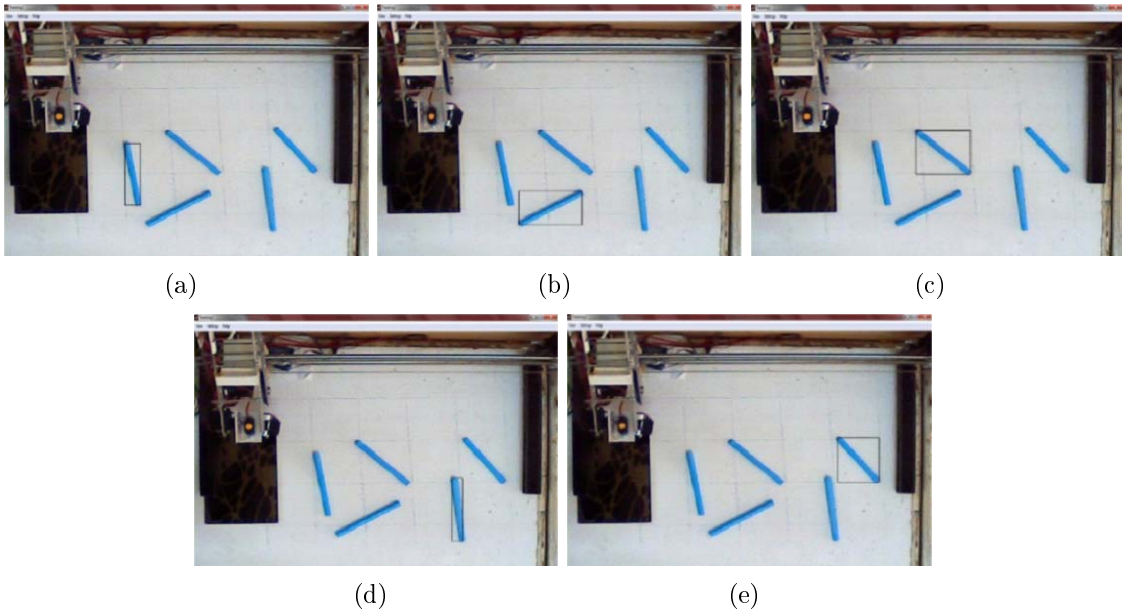

(a) (b) (c)

(d) (e)

FIGURE 12. Objects detected using the RGB-based algorithm

TABLE 2. Capsules position, orientation and inverse kinematics solutions

Image	From image			To robot				
	x (pixel)	y (pixel)	ψ (°)	θ_2 (°)	θ_3 (°)	θ_4 (°)	θ_5 (°)	d_1 (mm)
a	223	309	81.46	69.85	132.83	127.03	81.46	121.5
b	305	382	29.73	57.66	110.5	137.16	29.73	216.2
c	329	266	42.84	77.15	145.11	122	42.84	244
d	462	361	84.43	61.26	117.2	134	84.43	399.5
e	511	265	51.38	77.29	145.35	121.95	51.38	455.7

6. **Conclusion.** The study presented a vision control of 5-DOF arm robot based on RGB-filter to be used in grasping fallen Cobalt-60 model capsules. A model robot was designed and inverse kinematic equations were developed. Camera calibration was done using pin-hole camera model to form camera equations in x and y directions. The extrinsic and intrinsic parameters were extracted using MATLAB camera calibrator toolbox. Experiments were carried out to prove the system validity. The results showed that the robot arm had the ability to grasp the target objects and follow a sequence planned to

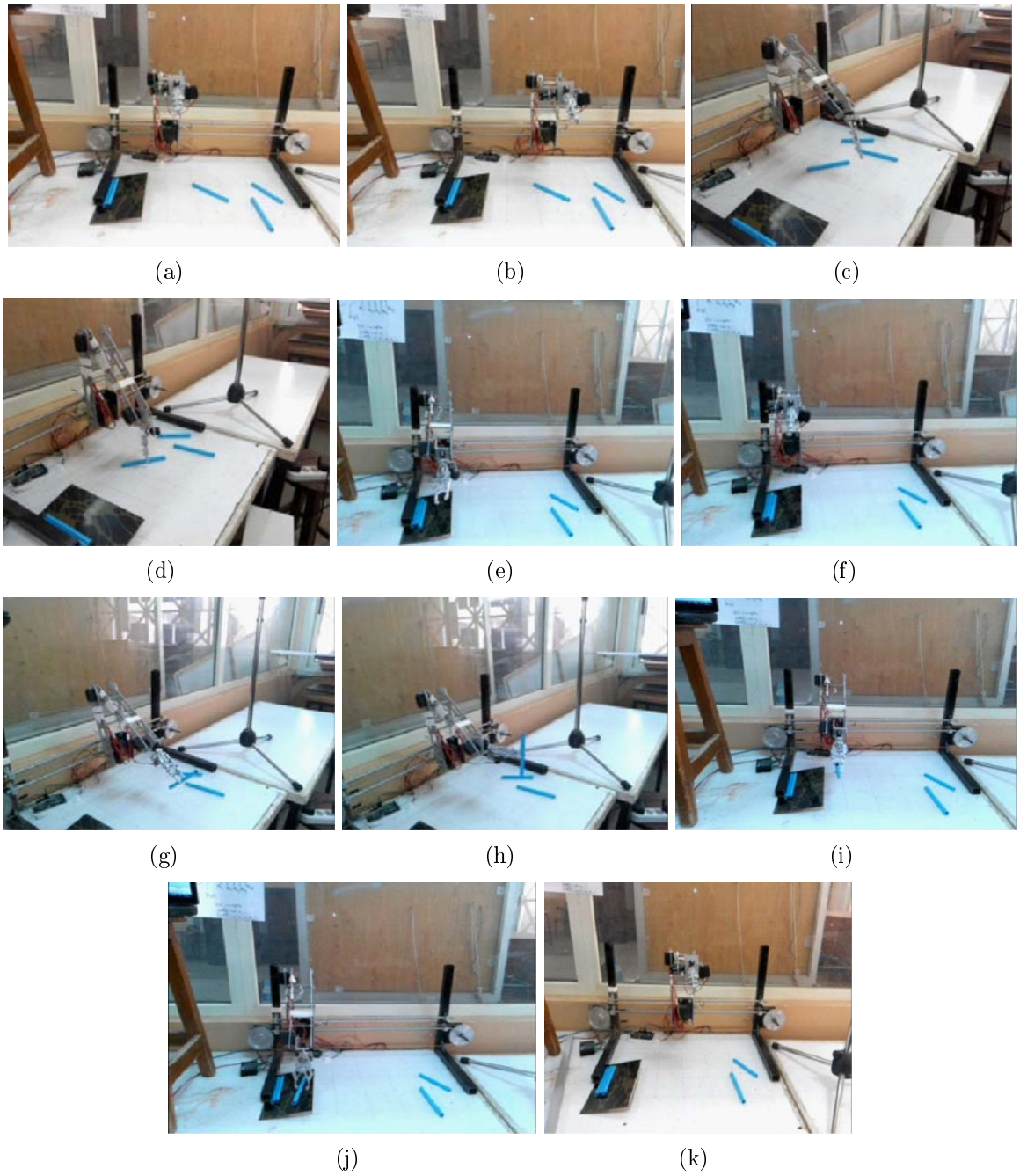

FIGURE 13. Robot arm detecting and grasping objects

collect all the fallen objects in a safe storage area. The work thus developed and reported in this paper sets the basis of design and developing of a prototype arm robot with a nuclear resistance capability to be used in the Cobalt-60 irradiators.

REFERENCES

[1] International Atomic Energy Agency, Gamma irradiators for radiation processing, *IAEA DGPF/CD*, Vienna, 2004.

[2] A. Barabanova, J. R. Croft and D. M. Delves, *The Radiological Accident in Soreq*, IAEA, Vienna, 1990.

[3] International Atomic Energy Agency, Radiation safety of gamma and electron irradiation facilities, *IAEA Safety Series No. 107*, Vienna, 1992.

[4] International Atomic Energy Agency, Practice specific model regulations: Radiation safety of non-medical irradiation facilities, *IAEA-TECDOC-1367*, Vienna, 2003.
[5] International Atomic Energy Agency, International basic safety standards for protection against ionizing radiation and for the safety of radiation sources, *IAEA Safety Series No. 115*, Vienna, 2011.
[6] K. Lauridsen, M. Decreton, C. C. Seifert and R. Sharp, *Reliability and Radiation Tolerance of Robots for Nuclear Applications*, Risoe National Lab., Systems Analysis, Roskilde, Denmark, 1996.
[7] R. L. Kress, *Category Archives*, American Nuclear Society, 2013.
[8] L. Lin, Y. Song, Y. Yang, H. Feng, Y. Cheng and H. Pan, Computer vision system R&D for EAST Articulated Maintenance Arm robot, *Fusion Engineering and Design*, vol.100, pp.254-259, 2015.
[9] M. Balter, A. Chen, T. Maguire and M. Yarmush, The system design and evaluation of a 7-DOF image-guided venipuncture robot, *IEEE Trans. Robot.*, vol.31, no.4, pp.1044-1053, 2015.
[10] M. Liu et al., Fast object localization and pose estimation in heavy clutter for robotic bin picking, *The International Journal of Robotics Research*, vol.31, no.8, pp.951-973, 2012.
[11] Y. Matsuda, K. Tsukamoto, T. Matsumoto, S. Goto, T. Sugi and N. Egashira, Remote operation system of robot arm with visual servo mechanism by target selection, *International Journal of Innovative Computing, Information and Control*, vol.10, no.4, pp.1381-1390, 2014.
[12] D. Ognibene and G. Baldassare, Ecological active vision: Four bioinspired principles to integrate bottom-up and adaptive top-down attention tested with a simple camera-arm robot, *IEEE Trans. Autonomous Mental Development*, vol.7, no.1, pp.3-25, 2015.
[13] A. Kazakidi, X. Zabulis and D. Tsakiris, Vision-based 3D motion reconstruction of octopus arm swimming and comparison with an 8-arm underwater robot, *IEEE International Conference on Robotics and Automation*, Seattle, pp.1178-1183, 2015.
[14] S. Sharma, A. Jaju, P. Pal and V. Sastry, Vision guided robotic stacking of pellets to a fixed length, *Proc. of Conference on Advances in Robotics*, New York, pp.1-6, 2013.
[15] S. Sanjeev, C. Shobhraj, P. Sibabrata and P. Prabir, Vision guided robotic handling for density measurement of fuel pellets, *Proc. of the National Conference on Machine Vision and Image Processing*, Pune, pp.97-101, 2011.
[16] J. Denavit and R. S. Hartenberg, A kinematic notation for lower-pair mechanisms based on matrices, *Journal of Applied Mechanics*, vol.77, pp.215-221, 1955.
[17] J. J. Craig, Introduction to robotics: Mechanics and control, *Pearson Education*, 3rd Edition, 2005.
[18] J. Kay, *Introduction to Homogeneous Transformations & Robot Kinematics*, Rowan University, Computer Science Department, 2005.
[19] M. Al-Faiz and M. Saleh, Inverse kinematics analysis for manipulator robot with wrist offset based on the closed-form algorithm, *International Journal of Robotics and Automation*, vol.2, no.4, 2011.
[20] J. Hallenberg, *Robot Tool Center Point Calibration Using Computer Vision*, Master Thesis, University of Linköpink, Sweden, 2007.
[21] A. Colomé, *Smooth Inverse Kinematics Algorithms for Serial Redundant Robots*, Master Thesis, Institut de Robotica i Informatica Industrial (IRI), Universit at Politecnica de Catalunya (UPC), Barcelona, Spain, 2011.
[22] H. Malm, *Studies in Robotic Vision, Optical Illusions and Nonlinear Diffusion Filtering*, Ph.D. Thesis, Lund University, 2003.
[23] J. Heikkilä and O. Silvén, A four-step camera calibration procedure with implicit image correction, *Proc. of the Conference on Computer Vision and Pattern Recognition*, San Juan, pp.1106-1112, 1997.
[24] Z. Zhang, A flexible new technique for camera calibration, *IEEE Trans. Pattern Analysis and Machine Intelligence*, vol.22, no.11, pp.1330-1334, 2009.
[25] MathWorks Company, *Single Camera Calibration App.*, http://in.mathworks.com/help/vision, 2013.
[26] E. Hemayed, A survey of camera self calibration, *Proc. of the IEEE Conference on Advanced Video and Signal Based Surveillance*, pp.351-357, 2003.